

Condensed phase isomerization through tunneling gateways

Alec Wodtke (✉ alec.wodtke@mpibpc.mpg.de)

Max Planck Institute for biophysical chemistry <https://orcid.org/0000-0002-6509-2183>

Amab Choudhury

Max Planck Institute for biophysical chemistry <https://orcid.org/0000-0002-5288-9468>

Jessalyn DeVine

Max Planck Institute for biophysical chemistry

Shreya Sinha

Dept. of Chemistry, University of Potsdam

Jascha Lau

Max Planck Institute for biophysical chemistry

Alexander Kandratsenka

Max Planck Institute for biophysical chemistry

Dirk Schwarzer

Max Planck Institute for Biophysical Chemistry <https://orcid.org/0000-0003-3838-2211>

Peter Saalfrank

University of Potsdam

Physical Sciences - Article

Keywords: tunneling gateways, heavy-atom condensed-phase tunneling, condensed phase isomerization

Posted Date: November 15th, 2021

DOI: <https://doi.org/10.21203/rs.3.rs-1052940/v1>

License:   This work is licensed under a Creative Commons Attribution 4.0 International License.

[Read Full License](#)

Condensed phase isomerization through tunneling gateways

Arnab Choudhury^{1,2}, Jessalyn A. DeVine², Shreya Sinha³, Jascha A. Lau^{1,2,a}, Alexander Kandratsenka², Dirk Schwarzer², Peter Saalfrank³ and Alec M. Wodtke^{1,2*}

¹Institute for Physical Chemistry, Georg-August University; Goettingen, Germany.

²Dept. of Dynamics at Surfaces, Max-Planck-Institute for biophysical Chemistry; Goettingen, Germany.

³Dept. of Chemistry, University of Potsdam, Potsdam, Germany

^aCurrent address: Department of Chemistry, University of California, Berkeley, California 94720, USA

*Corresponding author. Email: alec.wodtke@mpibpc.mpg.de.

Abstract: We observe that the orientational isomerization of CO on a NaCl(100) surface proceeds by thermally-activated tunneling between 19 and 24K. The rate constants of three isotopomers follow an Arrhenius temperature dependence, exhibiting activation energies below the reaction's predicted barrier height and anomalously small prefactors. In addition, the rates depend strongly on isotope, but non-intuitively on mass. A quantum rate theory of condensed-phase tunneling qualitatively explains these observations. Vibrationally excited states, accidentally close in energy but localized on opposite sides of the isomerization barrier, provide tunneling gateways between the isomers in a process that can be many orders-of-magnitude faster than rates predicted by commonly used semi-classical models. This suggests heavy-atom condensed-phase tunneling may be more important than currently assumed.

Quantum tunneling is the process by which a particle passes from one side of a potential barrier to the other, despite lacking the energy required to surmount it ¹. Though often ignored, tunneling may contribute significantly to the rates of chemical reactions with a barrier separating reactants from products, as all reactions are fundamentally quantum mechanical processes. Indeed, tunneling is included in chemical models of cold ($T \sim 10\text{--}50\text{K}$) interstellar clouds ^{2,3} postulated to be the birthplace of the “molecules of life” ⁴, and has been invoked to explain the rates of some important enzyme reactions at physiological temperatures ^{5–8}.

Experimentally, tunneling in chemical reactions is inferred by observing the influence of temperature T and isotope on the reaction rate constant $k(T)$. Over-the-barrier reactions are faster at elevated temperature due to the higher population of molecules in states with energies exceeding the barrier height. This generally follows the Arrhenius relation,

$$k(T) = A e^{-E_a/k_B T}. \quad (1)$$

Here, A and E_a are the Arrhenius prefactor and activation energy, respectively, and k_B is the Boltzmann constant. Tunneling, on the other hand, is often invoked to explain reactions whose rates become nearly temperature independent at low temperature—ground state tunneling ^{9,10}. Of course, vibrationally excited states that lie below the barrier may tunnel more rapidly than the ground state; hence, tunneling may also be thermally-activated and exhibit Arrhenius-like T -dependence. In such cases, tunneling can be identified by an anomalously small reaction prefactor—reflecting the small probability to tunnel through the barrier—and activation energies smaller than the expected barrier height for reaction ^{11,12}.

Tunneling is strongly mass-dependent; however, isotope-dependent reaction rates are not always indicative of tunneling. Isotopic exchange in over-the-barrier reactions can affect both A and E_a through changes in zero-point energies (ZPEs), which vary in a systematic manner with mass so that substitution with lighter isotopomers gives either faster (normal isotope effect) or slower (inverse isotope effect) reaction rates. The mass dependence of tunneling reactions is typically considered to arise from the decreased likelihood of transmission through a barrier for heavier particles, leading to large ‘normal’ isotope effects that are particularly pronounced for lighter elements. As such, the largest tunneling-induced isotope effects are seen for H/D/T substitution; for example, room temperature rates vary by a factor of 80 in Soybean Lipoxygenase-1 catalysis ⁸. In the largest isotope effect seen for tunneling of heavier atoms, $^{12}\text{C}^{16}\text{O}$ reacted $4 \times$ faster than $^{13}\text{C}^{16}\text{O}$ in a CO cascading process on a copper surface at $T < 6\text{K}$ ⁹.

Recently, it was found that when CO adsorbs at a NaCl(100) surface¹³⁻¹⁵, it may bind with the C-atom or the O-atom facing the surface^{16,17}. Subsequent theoretical work on the potential energy surface (PES) for this system has shown that the “O-down” isomer is $\sim 610\text{ cm}^{-1}$ higher in energy than the “C-down” structure, and must pass over a $\sim 570\text{ cm}^{-1}$ barrier to isomerize^{18,19}. Furthermore, the O-down isomer is longer lived when buried under additional CO suggesting that the isomerization barrier is slightly higher in buried monolayer samples.

Here, we show that the rates of conversion of O-down to C-down CO in buried monolayers of $^{12}\text{C}^{16}\text{O}$, $^{13}\text{C}^{16}\text{O}$, and $^{13}\text{C}^{18}\text{O}$ exhibit the fingerprints of thermally activated tunneling. The kinetic isotope effect (KIE) is large and remarkably, it is not the lightest isotopomer that tunnels most rapidly. We present a simple theory for condensed phase tunneling based on Fermi’s golden rule (FGR) that qualitatively reproduces the key experimental observations. The FGR model describes a phonon bath that induces transitions between a pair of vibrational states of the CO adsorbate, each localized on opposite sides of the barrier. The pair of states provides a gateway for accelerated tunneling.

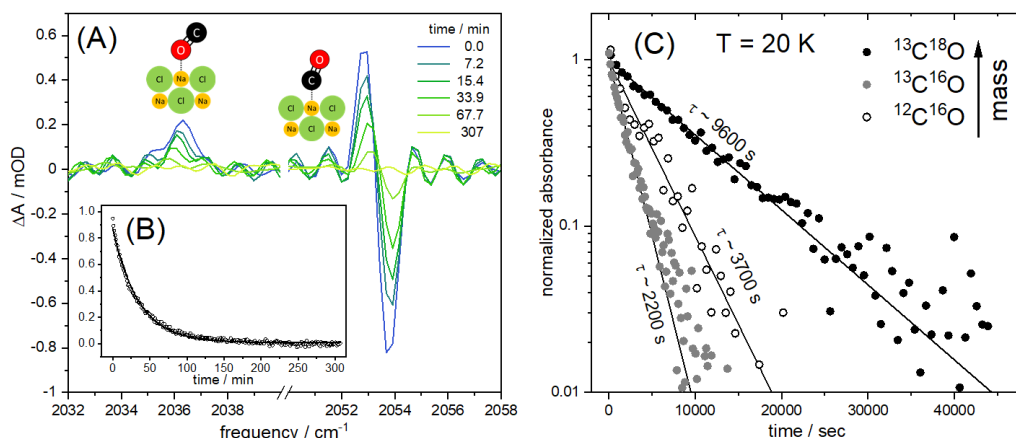


Figure 1: Observed kinetics of CO flipping reaction. (A) Difference absorbance FTIR spectra for a buried $^{13}\text{C}^{18}\text{O}$ monolayer at 21K following overlayer excitation. The line shape of the ca. 2053 cm^{-1} feature arises from a shift in the C-down center frequency, as neighboring O-down adsorbates convert to C-down. (B) The time dependent O-down concentration (o) derived from the spectra in panel (A) and exponential fit (—). (C) Example kinetic traces analogous to that shown in (B), for all three isotopes at $T = 20\text{K}$. Extracted decay lifetimes τ are also provided; note that the $^{12}\text{C}^{16}\text{O}$ isotopomer reacts more slowly than the heavier $^{13}\text{C}^{16}\text{O}$.

The full experimental procedure is described in section S1 (fig. S1) of the Supporting Information (SI). Briefly, a pulsed molecular beam is used to prepare a $^{13}\text{C}^{18}\text{O}$, $^{13}\text{C}^{16}\text{O}$, or $^{12}\text{C}^{16}\text{O}$ monolayer, which is subsequently buried beneath overlayers of $^{12}\text{C}^{16}\text{O}$ deposited with a second pulsed molecular beam. At a chosen temperature (19-24 K), infrared laser excitation produces populations of O-down CO far from equilibrium. The subsequent return to equilibrium is observed

using time-resolved Fourier-transform infrared (FTIR) spectroscopy to monitor the spectral signatures of each isomer ¹⁶.

Fig. 1A shows examples of FTIR spectra for a buried ¹³C¹⁸O monolayer following laser excitation of the ¹²C¹⁶O overlayers ¹⁷. Here, a reference IR absorption spectrum taken before excitation is subtracted from transient post-excitation spectra. The O-down isomer absorbs at ~2037 cm⁻¹ and disappears with time, while the depletion feature at ~2053 cm⁻¹ is due to C-down CO and recovers with time. Figure 1B shows the time-dependence of the O-down concentration obtained from the spectral data in Fig. 1A (section S2, figures S2-S7), along with an exponential fit that yields the observed characteristic decay time τ_{obs} (section S3, table S1).

Fig. 1C shows measured decays at 20 K for the three isotopomers, exhibiting a ~5× KIE. Remarkably, ¹²C¹⁶O reacts more slowly than ¹³C¹⁶O. Observations of such an enhancement of tunneling for heavier isotopes have been reported for H/D substitution, where the large difference in ZPE and average tunneling energy can lead to such an inverse dependence of the tunneling rate ²⁰; however, in the heavy-atom case considered here, the change in ZPE is only a few cm⁻¹, and thus such a mass dependence is quite unexpected.

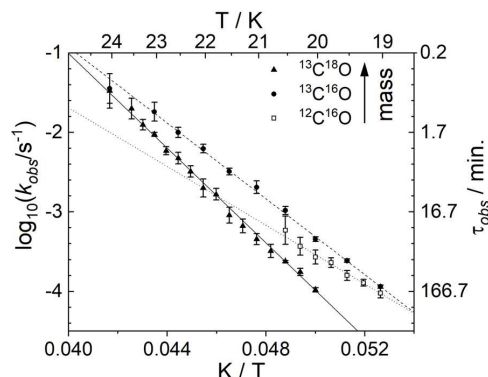


Figure 2: Isotope effect on flipping rates of metastable O-down CO on NaCl(100) in a buried monolayer. Arrhenius plot of the experimentally-derived rate constants for three isotopomers (symbols) and fits based on Eq. (1) (lines). Note that $k_{obs} = 1/\tau_{obs}$ and that since τ_{obs} varies by more than two orders of magnitude, the fits exhibit little correlation error between the derived values of A_{obs} and E_a^{obs} .

This mass effect is seen throughout the complete temperature range of these studies—see Figure 2, where we show the measured rate constants for all three isotopomers in an Arrhenius plot. Fitting Eq. (1) to $1/\tau_{obs}$ provides isotope-dependent Arrhenius constants A_{obs} and E_a^{obs} (Table 1). A_{obs} and E_a^{obs} increase with isotopomer mass, by factors of ~10⁴ and ~1.6, respectively. Notably, the derived values of E_a^{obs} are far lower than the expected barrier height of ca. ~570 cm⁻¹ from the PES of Ref. ¹⁹; this is a clear indication that the isomerization proceeds through a tunneling process.

We next compare the experimentally-derived isotope-dependent rate parameters to predictions of two well established rate theories—transition state theory (TST), applicable for over-the-barrier reactions, and Wentzel-Kramers-Brillouin (WKB) theory, commonly employed for tunneling

reactions. In both cases we have used the recently reported two-dimensional PES for CO flipping, which is parametrized in terms of the CO-surface separation (Z) as well as rotation of the CO molecule (θ)¹⁹.

Table 1: Arrhenius rate parameters for isotopically-selected CO flipping on NaCl(100) in a buried monolayer. All A -factors are in units of s^{-1} and all E_a -values are in units of cm^{-1} .

	Experiment [*]		TST [#]		FGR Rate Theory [†]		WKB CC ^{**}		WKB MEP ^{††}	
	A_{obs}	E_a^{obs}	A_{TST}	E_a^{TST}	A_{FGR}	E_a^{FGR}	A_{WKB}	E_a^{WKB}	A_{WKB}	E_a^{WKB}
¹² C ¹⁶ O	1×10^6	295 ± 30	1.19×10^{12}	501.6	6.9×10^5	231	3.2×10^8	427	1.9×10^9	444.2
¹³ C ¹⁶ O	4×10^8	380 ± 10	1.21×10^{12}	503.5	2.0×10^6	256	2.9×10^8	430	1.6×10^9	445.6
¹³ C ¹⁸ O	8×10^{10}	480 ± 10	1.22×10^{12}	505.6	9.5×10^6	304	1.4×10^8	428	6.0×10^8	441.6

^{*}obtained by performing an error-weighted fitting of Eq. (1) to the measured rate constants. Error bars reflect the 95% confidence intervals. [#]found by fitting the predictions of transition state theory to an Arrhenius expression; see section S4. [†]calculated as described in section S6. ^{**}obtained using a corner cutting tunneling path with 2D ZPE as described in section S5. ^{††}Obtained using the minimum energy tunneling path with 2D ZPE as described in section S5.

TST (section S4) predicts rate constants that, over the finite temperature range of these experiments, exhibit an Arrhenius temperature-dependence,

$$k_{TST}(T) = \frac{k_B T}{h} e^{-\Delta G^\ddagger(T)/k_B T} \cong A_{TST} e^{-E_a^{TST}/k_B T}. \quad (2)$$

Here, the mass dependence of the Gibbs free energy of activation, $\Delta G^\ddagger(T)$, determines how the choice of isotopomer influences E_a^{TST} and A_{TST} . Table 1 shows that both E_a^{TST} and A_{TST} are much larger than their experimentally-derived counterparts, and isotopic exchange from ¹²C¹⁶O to ¹³C¹⁸O changes A_{TST} and E_a^{TST} by less than 1%. The TST rate constants exhibit a normal KIE, where light isotopes react faster than heavy ones, thus failing to capture the peculiar mass dependence seen in experiment. The failure of TST to describe the experiment is not surprising, and is further evidence that the reactions observed in experiment proceed by tunneling.

We also calculated thermally activated tunneling rates based on the WKB formalism using both the minimum energy path (MEP) and a corner cutting (CC)²¹ tunneling path on the PES of Ref.¹⁹ (section S5). The WKB rates also exhibit an Arrhenius temperature dependence (Table 1, fig. S9 & table S2), and the activation energies are lower than those of TST, reflecting reactions occurring through tunneling. Like TST, WKB fails to describe the KIE seen in experiment. In contrast to observation, E_a^{WKB} is only weakly dependent on isotopomer, and A_{WKB} decreases with mass. This reflects the fact that WKB predicts that heavier isotopomers tunnel more slowly than lighter ones.

We pause here to emphasize three key experimental observations: (a) the derived values of E_a^{obs} are substantially below the theoretically-predicted barrier height¹⁹; (b) the derived values of A_{obs} are extraordinarily low relative to A_{TST} ; and (c) the KIE is large, with a seemingly erratic mass-dependence. These observations are explained by a tunneling mechanism hinging upon a

thermally-populated vibrationally-excited state of the O-down isomer that accidentally lies close in energy to a vibrationally-excited C-down state localized across the isomerization barrier. We envision that population is transferred from one state to the other by interactions with the environment, allowing the pair of quantum states to act as a gateway for tunneling. We then interpret the observed Arrhenius T -dependence as a reflection of the thermal population of the gateway ($e^{-E_a^{obs}/k_B T}$) and the intrinsic rate of tunneling through the gateway (A_{obs}).

This picture immediately allows us to understand the unexpected KIE. Although vibrational energy levels generally depend systematically on isotopic substitution, vibrational states localized on opposite sides of the barrier will be only accidentally close in energy. Hence, varying the isotope changes the gateway energy in a way that appears non-systematic. Viewing these results within the context of the gateway mechanism, a clear correlation is seen (Table 1), where A_{obs} increases dramatically with increasing E_a^{obs} ; this reflects the rapid increase in tunneling probability as the gateway's energy comes closer to that of the barrier. The fact that we can rationalize the KIE in this way strongly supports the gateway tunneling mechanism.

To investigate this mechanism at a more fundamental level, we developed a simple quantum rate theory of condensed-phase tunneling based on FGR (section S6). Here, we employ the PES of Ref. ¹⁹, solving the time-independent Schrödinger equation to obtain all vibrational eigenstates up to 1400 cm^{-1} above the C-down ZPE for all three isotopomers. These states define a 2D system in perturbative contact with a bath of phonon states, produced by low frequency motions of the CO monolayer (*e.g.* hindered translations and rotations) and the NaCl solid (fig. S10). We then compute thermal rates for population transfer between all O-down localized states to all C-down localized states using FGR to describe the phonon-bath-induced perturbative coupling between system states.

The FGR model predicts rate constants that obey an Arrhenius law similar to that seen in experiment (Figure 3A and Table 1). In contradiction to WKB and TST, but in agreement with experiment, it also predicts that A_{FGR} increases with mass. In addition, it exhibits an analogous correlation between A_{FGR} and E_a^{FGR} to that seen in experiment. Finally, both A_{FGR} and E_a^{FGR} are strongly dependent on isotopomer in contrast to both TST and WKB. Notably, the FGR model confirms the proposition that tunneling occurs through quantum gateways. Inspection of the state-to-state rate constants (fig. S11) reveals that thermal tunneling is dominated by population-transfer between specific pairs of vibrationally excited states located close enough in energy to be coupled by absorption or emission of a single phonon. The vibrational wavefunctions involved in the

tunneling gateway are highly localized either on the C-down or the O-down side of the barrier and possess significant rotational excitation as reflected in their nodal structure (Fig. 3B-D).

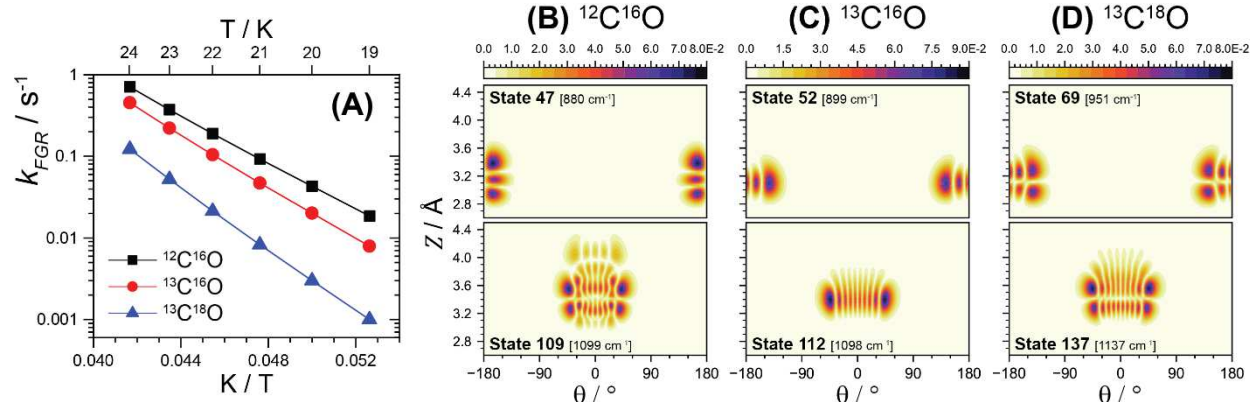


Figure 3. Thermal rates of condensed-phase tunneling of CO on NaCl(100) based on the FGR theory calculations. (A) The temperature dependence of the rate constants. (B-D) Square root of the probability amplitudes describing the quantum-gateways dominating calculated tunneling rates for (B) $^{12}\text{C}^{16}\text{O}$, (C) $^{13}\text{C}^{16}\text{O}$, and (D) $^{13}\text{C}^{18}\text{O}$. In each panel, the angle of CO with respect to the surface normal (θ) is the horizontal axis, where $\theta=0^\circ$ represents the C-O bond parallel to the surface normal in the C-down configuration. The vertical axis is the distance of the CO molecule from the surface (Z). State energies are given relative to the classical C-down minimum in the PES.

We also used the FGR tunneling model to calculate ground-state tunneling rates, $k_{\text{FGR}}(T = 0\text{K})$ (Table 2). The predicted rates are six orders-of-magnitude smaller than those for $T \sim 20\text{K}$, consistent with an experimentally-determined upper-limit to the ground state rate constant (section S7) and with the fact that thermally-activated tunneling dominates for $19\text{K} < T < 24\text{K}$. We highlight the FGR model's prediction that at $T = 0\text{K}$, $^{13}\text{C}^{16}\text{O}$ reacts faster than $^{12}\text{C}^{16}\text{O}$, an inverse mass-dependence in the ground state tunneling rates reminiscent of that seen in experiment. Corresponding ground-state WKB rates (Table 2) appear with the normal mass dependence. Remarkably, the WKB treatment of tunneling along the minimum-energy pathway underestimates the ground state rate of tunneling by 7-9 orders of magnitude ($k_{\text{WKB-MEP}}$) and still by 4-6 orders of magnitude when assuming corner cutting ($k_{\text{WKB-CC}}$). We consider these WKB rates to be upper limits, as we have employed the ZPE of both the Z and θ coordinates.

Table 2. Tunneling rates for ground-state CO back flipping on NaCl(100).

	ZPE (meV)*	$k_{\text{WKB-MEP}} (\text{s}^{-1})^{**}$	$k_{\text{WKB-CC}} (\text{s}^{-1})^{\#}$	$k_{\text{FGR}} (\text{s}^{-1})$	$k_{\text{obs}} (\text{s}^{-1})$
$^{12}\text{C}^{16}\text{O}$	8.18	2.5×10^{-16}	2.4×10^{-13}	1.4×10^{-9}	
$^{13}\text{C}^{16}\text{O}$	8.07	5.5×10^{-17}	5.8×10^{-14}	1.5×10^{-9}	
$^{13}\text{C}^{18}\text{O}$	7.84	7.2×10^{-18}	9.9×10^{-15}	4.0×10^{-9}	$3.0 \times 10^{-8}^{\dagger}$

*The two dimensional zero point energy. **Calculated for the minimum energy path between reactant and product (section S5). $^{\#}$ Calculated along a corner cutting pathway where the tunneling distance was minimized (section S5). † Upper limit.

In past descriptions of thermally-activated condensed phase tunneling, a semiclassical picture was adopted involving fluctuating solvent modes that alter the shape of the reaction path²² for

example by lowering the average barrier height or tunneling distance ⁷. The observations of this work reveal a conceptually different picture, where condensed phase tunneling occurs due to environmental fluctuations that induce transitions between bound-states localized on opposite sides of an isomerization barrier. Consequently, the energy differences between product and reactant states, as well as the character of their wavefunctions, critically influence transition probabilities. Because of this, quantum gateways enhance tunneling rates in a way that cannot be described by theories treating tunneling as a scattering problem involving continuum states.

The tunneling seen in this work is unexpectedly efficient, as the quantum gateways act as leaky holes through the reaction barrier, allowing for accelerated reaction rates. If the gateways could be closed, the rate of tunneling would be significantly reduced. This is similar to the effect of resonant tunneling of electrons in condensed phases ²³⁻²⁹, but with heavy atoms. Tunneling through quantum gateways is easily understood through a simple quantum rate model in the uniquely informative CO/NaCl(100) system; in larger systems exhibiting tunneling at higher temperatures, the number of resonances may become larger, yet the fundamental picture is likely to remain the same. Further developing the condensed phase tunneling theory described here is clearly an exciting future prospect arising from this work. We see no reason, in principle, why such an FGR model cannot be applied to thermally-activated tunneling reactions in enzymes, for example.

More specifically, we have shown in the CO back-flipping reaction that tunneling gateways can lead to reaction rates that are faster than expected. This may be of particular relevance to interstellar chemistry. Long thought to be dominated by gas-phase ion-molecule reactions that lack an activation barrier ³⁰, it has more recently become apparent that reactions with barriers may take place by tunneling on and in ices deposited on dust grains ³¹. Neglecting the influence of quantum gateways may result in severe underestimations of actual tunneling rates.

References

- 1 Hund, F. Zur Deutung der Molekelspektren. I. *Zeitschrift für Physik* **40**, 742-764 (1927).
- 2 Hasegawa, T. I., Herbst, E. & Leung, C. M. Models of gas-grain chemistry in dense interstellar clouds with complex organic molecules. *The Astrophysical Journal Supplement Series* **82**, 167-195 (1992).
- 3 Hiraoka, K., Sato, T. & Takayama, T. Interstellar chemistry - Tunneling reactions in interstellar ices. *Science* **292**, 869-870 (2001).
- 4 Pizzarello, S. & Huang, Y. S. The deuterium enrichment of individual amino acids in carbonaceous meteorites: A case for the presolar distribution of biomolecule precursors. *Geochimica Et Cosmochimica Acta* **69**, 599-605 (2005).
- 5 Grant, K. L. & Klinman, J. P. Evidence that both protium and deuterium undergo significant tunneling in the reaction catalyzed by bovine serum amine oxidase. *Biochemistry* **28**, 6597-6605 (1989).
- 6 Cha, Y., Murray, C. & Klinman, J. Hydrogen tunneling in enzyme reactions. *Science* **243**, 1325-1330 (1989).

- 7 Bruno, W. J. & Bialek, W. Vibrationally enhanced tunneling as a mechanism for enzymatic hydrogen transfer. *Biophysical Journal* **63**, 689-699 (1992).
- 8 Knapp, M. J., Rickert, K. & Klinman, J. P. Temperature-dependent isotope effects in Soybean Lipoxxygenase-1: Correlating hydrogen tunneling with protein dynamics. *Journal of the American Chemical Society* **124**, 3865-3874 (2002).
- 9 Heinrich, A. J. Molecule cascades. *Science* **298**, 1381-1387 (2002).
- 10 Lin, C., Durant, E., Persson, M., Rossi, M. & Kumagai, T. Real-space observation of quantum tunneling by a carbon atom: Flipping reaction of formaldehyde on Cu(110). *The Journal of Physical Chemistry Letters* **10**, 645-649 (2019).
- 11 Klinman, J. P. & Offenhacher, A. R. Understanding biological hydrogen transfer through the lens of temperature dependent kinetic isotope effects. *Accounts of Chemical Research* **51**, 1966-1974 (2018).
- 12 Carpenter, B. K. Heavy-atom tunneling as the dominant pathway in a solution-phase reaction? Bond shift in antiaromatic annulenes. *Journal of the American Chemical Society* **105**, 1700-1701 (1983).
- 13 Schmicker, D., Toennies, J. P., Vollmer, R. & Weiss, H. Monolayer structures of carbon monoxide adsorbed on sodium chloride: A helium atom diffraction study. *The Journal of Chemical Physics* **95**, 9412-9415 (1991).
- 14 Heidberg, J., Kampshoff, E. & Suhren, M. Correlation field, structure, and phase transition in the monolayer CO adsorbed on NaCl(100) as revealed from polarization Fourier-transform infrared spectroscopy. *The Journal of Chemical Physics* **95**, 9408-9411 (1991).
- 15 Chen, L., Lau, J. A., Schwarzer, D., Meyer, J., Verma, V. B. & Wodtke, A. M. The Sommerfeld ground-wave limit for a molecule adsorbed at a surface. *Science* **363**, 158-161 (2019).
- 16 Lau, J. A., Choudhury, A., Li, C., Schwarzer, D., Verma, V. B. & Wodtke, A. M. Observation of an isomerizing double-well quantum system in the condensed phase. *Science* **367**, 175-178 (2020).
- 17 Lau, J. A., Chen, L., Choudhury, A., Schwarzer, D., Verma, V. B. & Wodtke, A. M. Transporting and concentrating vibrational energy to promote isomerization. *Nature* **589**, 391-395 (2021).
- 18 Chen, J., Hariharan, S., Meyer, J. & Guo, H. Potential energy landscape of CO adsorbates on NaCl(100) and implications in isomerization of vibrationally excited CO. *The Journal of Physical Chemistry C* **124**, 19146-19156 (2020).
- 19 Sinha, S. & Saalfrank, P. "Inverted" CO molecules on NaCl(100): A quantum mechanical study. *Physical Chemistry Chemical Physics* **23**, 7860-7874 (2021).
- 20 Kohen, A. & Klinman, J. P. Enzyme Catalysis: Beyond Classical Paradigms. *Accounts of Chemical Research* **31**, 397-404 (1998).
- 21 Marcus, R. A. & Coltrin, M. E. A new tunneling path for reactions such as $H+H_2 \rightarrow H_2+H$. *The Journal of Chemical Physics* **67**, 2609-2613 (1977).
- 22 Klinman, J. P. & Kohen, A. Hydrogen Tunneling Links Protein Dynamics to Enzyme Catalysis. *Annual Review of Biochemistry* **82**, 471-496 (2013).
- 23 Chang, L. L., Esaki, L. & Tsu, R. Resonant tunneling in semiconductor double barriers. *Applied Physics Letters* **24**, 593-595 (1974).
- 24 Ricco, B. & Azbel, M. Y. Physics of resonant tunneling. The one-dimensional double-barrier case. *Physical Review B* **29**, 1970-1981 (1984).
- 25 Eisenstein, J. P., Pfeiffer, L. N. & West, K. W. Field-induced resonant tunneling between parallel two-dimensional electron systems. *Applied Physics Letters* **58**, 1497-1499 (1991).
- 26 Mengesha, M., Koshvaya, S. & Mal'nev, V. THz Radiation under Tunneling in Asymmetric Double Quantum Wells. *Journal of Electromagnetic Analysis and Applications* **03**, 271-276 (2011).
- 27 Sirtori, C., Capasso, F., Faist, J., Hutchinson, A. L., Sivco, D. L. & Cho, A. Y. Resonant tunneling in quantum cascade lasers. *IEEE Journal of Quantum Electronics* **34**, 1722-1729 (1998).
- 28 Capasso, F., Mohammed, K. & Cho, A. Resonant tunneling through double barriers, perpendicular quantum transport phenomena in superlattices, and their device applications. *IEEE Journal of Quantum Electronics* **22**, 1853-1869 (1986).
- 29 Stipe, B. C., Rezaei, M. A. & Ho, W. Single-molecule vibrational spectroscopy and microscopy. *Science* **280**, 1732-1735 (1998).
- 30 Winnewisser, G. & Herbst, E. Interstellar-molecules. *Rep. Prog. Phys.* **56**, 1209-1273 (1993).
- 31 Shannon, R. J., Blitz, M. A., Goddard, A. & Heard, D. E. Accelerated chemistry in the reaction between the hydroxyl radical and methanol at interstellar temperatures facilitated by tunnelling. *Nature Chemistry* **5**, 745-749 (2013).

Acknowledgments: The authors would like to thank Prof. Dr. Claus Ropers for helpful discussions.

Funding:

Alexander von Humboldt post-doctoral fellowship (JAD)

5 Max Planck Society for the Advancement of Science

Author contributions:

Conceptualization: AMW

Methodology: DS, JAL, JAD, AC

Investigation: AC, JAD

10 Computation: PS, SS, AK

Writing – original draft: AC, DS

Writing – review & editing: AMW, JAD

Competing interests: Authors declare that they have no competing interests.

15 **Data and materials availability:** All data are available in the main text or the supplementary materials.

Supplementary Materials

Experimental Methods (Section S1)

Supplementary Text (Sections S2-S7)

Figs. S1-S12

20 Tables S1-S2

References (32-38)

Supplementary Files

This is a list of supplementary files associated with this preprint. Click to download.

- [COLifetimeonNaClburiedMLNatureSI.docx](#)